J-Researchers

Journal of Civil Engineering Researchers

Journal homepage: www.journals-researchers.com

Simplified Unified Model for Flexural Capacity of Ductile HPC Beams with A Low Reinforcement Ratio

Wisam Hamad,[a] Mehdi Dehestani,[a,*]

[a] *Faculty of Civil Engineering, Babol Noshirvani University of Technology, Babol, Postal Box: 484, Postal Code: 47148-71167. Iran*

ABSTRACT

There is no specific model to predict the flexural capacity of high-performance concrete (HPC) beams with a low reinforcement ratio. Accordingly, a comprehensive experimental database containing 162 datasets was gathered from literature to propose an explicit analytical model containing various critical features, including fiber volume fraction, fiber aspect ratio, fiber strength, water-to-binder (w/b) ratio of mixture, and reinforcement ratio. Additionally, a supplementary experimental study involving a large-scale ductile HPC beam with a very low reinforcement ratio (almost negligible) was conducted to verify the model's performance. The findings revealed that the proposed bending model achieved an integral of absolute error (IAE) of 10.8% and a coefficient of variation (COV) of 1.04, indicating its high accuracy in comparison to a comprehensive experimental dataset comprising 162 large-scale beam tests. Furthermore, the comparison between the experimental results of the tested beam and the proposed model showed a deviation of 4.5%, which supports the effectiveness of the flexural capacity formulation. A parametric statistical analysis was conducted using Minitab software to evaluate the influence of key parameters affecting the roles of fiber and matrix.

ARTICLE INFO

Received: June 10, 2025
Accepted: August 02, 2025

Keywords:
Beam
HPC
Flexural Capacity
Low Reinforcement Ratio
Fiber Role

DOI: 10.61186/JCER.7.3.1
DOR: 20.1001.1.2538516.2025.7.3.1.1

1. Introduction

How reliable is using a high-performance concrete (HPC) beam containing a high-volume fraction of fibers as an independent RC member using a low reinforcement ratio, almost negligible? Researchers have raised this question since the first day the HPC and UHPC concrete generation was introduced, but it has not been thoroughly investigated due to concerns about the ductility of these beams. Although many experimental works concentrated on this context, there is almost no reliable model to predict the flexural capacity of such economic beams using UHPC and a minimal reinforcement ratio.

Investigations into the flexural characteristics of HPC (high-performance concrete), ultra-high performance concrete (UHPC), and engineered cementitious composites (ECC) beams with low reinforcement ratios have made significant progress over the last decade, uncovering crucial insights into their structural behavior and mechanisms for controlling cracking. In this context, Yang et al. [1] demonstrated that large-scale steel fiber-reinforced UHPC beams (L=2.9m) with reinforcement

* Corresponding author. Tel.: +989113136113; e-mail: dehestani@nit.ac.ir.

ratios ranging from 0 to 0.02 exhibit enhanced ductility, with ductility indices between 1.60 and 3.75, and that the method of placing UHPC influences fiber orientation and flexural performance. They used 2.0% volume fraction straight steel fibers within UHPC mixture with a water-to-binder (w/b) of 0.2 and a compressive strength range of 190.9-193.4 MPa. Meda et al. [2] explored fiber-reinforced concrete beams under flexure and noted that while fibers generally enhance post-cracking stiffness and toughness, in some cases, especially with low strain-hardening steel reinforcement and high toughness fibers, the overall rotation capacity and ductility may be reduced due to strain localization at cracks. They considered L=4.0m large-scale fiber-reinforced concrete beams with reinforcement ratio ranging from 0.0075 to 0.012 and compressive strengths of 43.2-49.7 MPa. They used various volume fractions of hook-ended steel fibers ranging from 0 to 0.76% within concrete with w/b=0.48. Kamal et al. [3] concentrated on ultra-high-strength concrete beams (L=1.0 m) containing various fiber types (polypropylene fibers and steel) with a volume fraction of 0-0.5% within the concrete mixture with w/b=0.3. They found that fibers increase the number of cracks and stiffness, reduce the crack width, and improve the ultimate load, underscoring the superior performance of steel fibers over polypropylene fibers in flexural strength enhancement. They selected a range of 0.012-0.017 for the reinforcement ratio of beams with compressive strength of around 130 MPa. Abbas et al. [4] investigated how the length and amount of steel fibers affect the mechanical properties of UHPC, highlighting that shorter steel fibers enhance flexural performance and that a higher dosage of fibers boosts both strength and resistance to chloride penetration. Accompanying these findings, Yoo et al. [5] combined experimental and numerical analyses of UHPFRC beams (L=3.5 m) with low reinforcement ratios (0 to 0.0171), confirming that increasing reinforcement ratio enhances post-cracking stiffness and load capacity, while crack patterns remain consistent, and emphasizing the importance of tension-softening behavior for accurate structural predictions. They used 2.0% straight steel fibers within concrete with w/b=0.2 and compressive strength of 196.7 MPa. They reported ductility indices ranging from 3.65 to 5.12 for their large-scale beams containing a very low reinforcement ratio. Yoo and Moon [6] assessed the flexural behavior of standard RC beams with L=3.0 m, very low reinforcement ratios of 0.178%–0.406 %, and incorporated hooked-end steel fibers (0.25%–1.0 % by volume). Although the addition of fibers enhanced post-cracking stiffness and cracking performance, it led to a decrease in ductility indices (from 8.3 to 2.2) and did not recover ultimate load losses caused by diminished rebar ratios. The research concluded that steel fibers at or below 1% cannot substitute for longitudinal rebars in providing ductility or strength margins. The study conducted by Cardoso et al. [7] examined the flexural performance of large-scale steel fiber-reinforced RC beams that had low reinforcing ratios, utilizing both experimental and analytical methods, with L=1.20 m and reinforcement ratios of 0.0028-0.007%. The concrete mixtures included hooked-end steel fibers with volume fractions ranging from 0.5% to 2.0%. Their compressive strength of the high-strength concrete matrices varied between 76.3 MPa and 95.2 MPa. Although their results demonstrated that RC beams with high volume fraction displayed notable capacity improvements (21–109%) when compared to plain RC beams, along with narrower crack widths at equivalent rebar stresses, employing fibers resulted in crack localization and diminished ductility, especially in beams with lower reinforcing ratios. Parvin et al. [8] conducted an experimental study on the flexural performance of UHPFRC beams reinforced with reinforcement ratio ranging from 0.64% to 1.45%, alongside a 2.0% volume fraction of hooked-end steel fibers. The UHPFRC attained a compressive strength of 130 MPa. The findings revealed that GFRP-reinforced beams had a greater load capacity (up to a 65% increase at lower reinforcement ratios) compared to their steel-reinforced equivalents, yet the fibers had a limited impact on reducing the brittle failure in GFRP samples. An increase in reinforcement ratios led to a change in failure modes from flexural to shear in GFRP beams, while steel-reinforced beams exhibited a ductile response.

While extensive experimental investigations have focused on large-scale fiber-reinforced concrete beams featuring low reinforcement ratios, there remains a notable absence of specific studies that reliably predict the flexural strength of such beams. To address this gap, the present study aims to compile a thorough database of experimental results encompassing a range of advanced concrete types, including HPC, UHPC, ECC, and various fiber-reinforced beams with a high-volume fraction of fibers. A total of 162 datasets were collected from the literature. In conjunction with this database, a rigorous supplementary experimental program was undertaken to validate the accuracy and reliability of the proposed unified flexural model. Furthermore, a detailed parametric study was incorporated to explore the pivotal role that fibers play in enhancing the bending moment capacity of these beams, effectively compensating for the limitations posed by lower reinforcement ratios. The main research hypothesis and novelty are proposing a new model for the flexural capacity of ductile HPC using separate equations for Msteel, Mfiber, and Mmatrix. Almost no specific study has distinguished the main role of fibers and matrix in the total bending moment capacity of HPC. As fiber and matrix play important roles in the case of a low (almost negligible) reinforcement ratio, their role should be precisely

recognized. Accordingly, the main novelty of the present study is to achieve a new reliable model to determine how much percentage of total bending moment that can be tolerated only through using fiber and matrix within HPC to compensate for the role of longitudinal reinforcement.

Table 1.
Details of the experimental database were collected from the literature to achieve the model

Reference	w/b	Powder	Fiber type	V_f (%)	f_c' (MPa)	ρ_s (-)	L (mm)	$b \times h$ (mm)	n
Yang et al. [1]	0.20	SF	straight steel	2.0	~ 194	0-0.0196	2900	180×270	13
Meda et al. [2]	0.48	-	hook-ended steel	0-0.76	~ 46.8	0.0075-0.015	4000	200×300	7
Kamal et al. [3]	0.30	SF	PP and steel	0-0.5	~ 130	0.012-0.017	1000	100×150	6
Yoo and Yoon [10]	0.13-0.14	SF+silica flour	smooth and twisted steel	0-2.0	~212.8	0.0094-0.015	2500	150×220	10
Yoo et al. [5]	0.20	SF	straight steel	2.0	~ 196.7	0-0.0171	2900	200×270	4
Singh et al. [11]	0.14	SF	hook-ended steel	2.25	~ 140	0.0175-0.0231	3500	250×250 150×150	3
Yoo and Moon [6]	0.37	-	hook-ended steel	0-1.0	~43.2	0.0018-0.0041	3000	320×300	40
Hasgul et al. [12]	0.18	SF+ GGBFS	straight micro-steel	0-1.5	~149.8	0.009-0.043	2500	150×250	8
Gümüş and Arslan [13]	0.17	SF	chopped carbon fiber and hooked-end steel	0-0.99	~116.4	0.0017-0.005	1300	150×200	18
Liu et al. [14]	0.32	FA	PVA fiber	0-2.0	~56	0.0128-0.0168	1700	120×200	8
Turker et al. [15]	0.18	SF+ GGBFS	short-straight and long hooked steel	0-1.5	~155.7	0.009-0.043	2500	150×200	12
Cardoso et al. [7]	0.26	SF+FA	hooked-end fibers	0-2	~81.5	0.0028-0.007	1200	150×150	9
Conforti et al. [16]	-	-	hooked-end steel and crimped glass, and embossed polymer	0-1.05	~48	0.005-0.012	900	150×150	14
Chen et al. [17]	0.20	SF+SFP	PP and steel	0-1.0	~136.1	0.0106	1500	150×200	2
Jin et al. [18]	-	-	PP	0-2.0	~29.43	0-0.0165	1100	100×120	5
Parvin et al. [8]	0.15	-	hooked-end steel	2.0	~130	0.0064-0.0145	1650	250×300	3

* w/b= water-to-binder ratio; n=number of database for each reference; V_f=volume fraction (%); ρ_s=reinforcement ratio; L=total length of large-scale beams; SF=silica fume powder; GGBFS=Ground granulated blast-furnace slag powder; FA=fly ash powder; "~" denotes the average compressive strength for each reference; PP=Polypropylene fibers; PVA= Polyvinyl alcohol fibers; "-" denotes unmentioned values in the references.

Table 2.
Details of the input variables for achieving the proposed model

Input	Count	Mean	Std. Dev.	Min	Max
V_f	162	0.89	0.77	0	2.25
f_c'	162	101.54	60.77	29.04	232.1
ρ_s	162	0.0096	0.0088	0	0.043
b	162	196.54	76.43	100	320
h	162	235.35	58.29	120	300
d	162	191.06	68.080	25	260
L	162	2255.66	892.96	900	4000
f_y rebar	162	507.66	41.32	386.3	602.8
fiber strength	162	1359.59	945.05	0	3800

2. Proposed Analytical Model

To develop and validate the proposed flexural strength model, an extensive database comprising 162 large-scale experimental beam specimens was compiled from the literature, which is comprehensively described in Table 1. The database includes RC beams constructed with HPC, UHPC, and ECC, all featuring low or very low longitudinal reinforcement ratios and varying fiber contents. The key parameters extracted and analyzed include fiber properties (volume fraction (V_f), aspect ratio, and strength), concrete compressive strength (f_c'), reinforcement ratio (ρ_s), and beam geometrical and mechanical properties. The V_f Ranged from 0% to 2.25%, with an average of 0.89%, capturing both non-fibered and highly fibered specimens. The concrete compressive strength spanned a wide range, from 29.04 MPa to 232.1 MPa, with a high mean of 101.54 MPa, confirming the inclusion of both HPC and UHPC

specimens. The reinforcement ratio varied between 0% and 4.3%, with an average of just 0.96%, reflecting the primary focus of this study on lightly reinforced members. In terms of geometry, beam widths ranged from 100 mm to 320 mm (mean: 196.5 mm), and heights from 120 mm to 300 mm (mean: 235.35 mm), encompassing both moderate and large cross-sections typical of structural-scale elements. This wide variation in mechanical properties, fiber contents, and cross-sectional dimensions ensures that the proposed model is robust, generalizable, and applicable across a broad spectrum of ductile HPC design scenarios, particularly those where minimizing steel reinforcement is desired while maintaining structural performance. The main similar properties of studies mentioned in Table 1 are the high volume fraction of fibers, low and very low (almost negligible) content of longitudinal reinforcement, and high quantity of powders used in concrete compositions. Also, the authors selected only studies containing large-scale beams under a four-point bending test, so that constant and similar boundary and load conditions were considered in the gathered database. Additionally, the experimental beams in the gathered database experienced only flexural failure, meaning that the shear failure was prevented using sufficient shear reinforcement (stirrups). The main question which needs to be addressed by this gathered experimental database is how much does fibers can be play the main role of reinforcement. For checking the range of low reinforcement ratio, various concrete design codes were used in the present study including (a) ACI 318-19 with $\rho_{min} = max\{(0.25\sqrt{f_c'}/f_y)\ and\ (1.4/f_y)\}$; (b) Eurocode 2 with $\rho_{min} = max\{(0.26f_{ctm}/f_y)\ and\ 0.0013\}$; (c) CSA A23.3 with $\rho_{min} = 0.2f_c'/f_y$; (d) IS 456 with $\rho_{min} = 0.85f_c'/f_y$; and (e) fib Model Code 2010 with $\rho_{min} = max\{(k_c f_{ct.cff}/f_{yd})\ and\ 0.0013\}$ where $k_c \approx 0.6 - 0.8$ and $f_{yd} = f_y/\gamma_s$. The analysis depicted that all (100%) the gathered database have reinforcement ratio lower than the minimum value recommended by Eurocode 2, CSA A23.3, IS 456, and fib Model Code 2010. However, ACI 318-19 recommends a more unconservative model than other deign codes. The details of input variables are summarized in Table 2. In the proposed flexural strength model tailored for ductile HPC beams with low or very low reinforcement ratios and approximately 2.0% steel fiber content, the total bending capacity is conceptualized as the sum of three distinct contributions: Msteel, Mfiber, and Mmatrix.

This decomposition is not only physically intuitive but also reflects the complex, multi-scale load-bearing behavior of ductile HPC. First, Msteel accounts for the conventional tensile reinforcement provided by steel bars, which remains essential but is purposefully minimized in this category of structural elements. The inclusion of Mfiber represents the tensile contribution of dispersed steel fibers within the matrix, introduced specifically to compensate for the reduced volume of rebar and to enhance crack-bridging capacity and post-cracking ductility. This is particularly critical in ductile HPC, where fibers are not supplementary but rather serve as a strategic reinforcement component. The third component, Mmatrix, captures the residual tensile resistance provided by the ductile HPC matrix itself, which, unlike ordinary concrete, exhibits significant tensile capacity due to its extremely low water-to-binder ratio (typically 0.17–0.19), high binder content, dense microstructure, and improved bond characteristics. This intrinsic matrix strength can contribute meaningfully to flexural behavior before cracking and in the early stages of crack development. Including Mmatrix is therefore critical for accurately capturing the contribution of the ductile HPC matrix, especially in mixes where the synergy between fine powders, silica fume, and low porosity leads to a measurable tensile stress capacity. Together, these three components provide a comprehensive and realistic representation of the load-resisting mechanism in ductile HPC beams with minimal reinforcement, supporting both predictive accuracy and physical interpretation. As shown in Eq. (1), this model was developed to predict the flexural capacity of reinforced concrete (RC) beams made with ductile HPC or UHPC, particularly in configurations where steel reinforcement is limited (i.e., low or very low reinforcement ratio). The model decomposes the total bending moment capacity into three distinct contributions:

$$M_n = M_{steel} + M_{fiber} + M_{matrix} \quad (1)$$

where M_{steel}, M_{fiber}, and M_{matrix} Represent the portion of reinforcement ratio, fiber, and matrix in the flexural capacity of ductile HPC beams with low or very low reinforcement ratio $(\rho_s \sim 0)$. In the first step, the portion of reinforcement for calculating flexural capacity can be measured by Eq. (2), as follows:

$$M_{steel} = A_s f_y \left(d - \frac{a}{2}\right) \quad (2)$$

where $A_s = \rho_s bd$ Is the area of tensile steel reinforcement (mm^2), b is the beam width (mm), d is the effective depth of the beam (mm), f_y is the yield strength of reinforcement (MPa), a is equivalent stress block depth (mm). In the second step, the fiber portion of the flexural capacity calculation needs to be measured using Eq. (3). In traditional reinforced concrete beams, the tensile capacity is primarily provided by steel reinforcement bars. However, when the reinforcement ratio is low or very low, reinforcement alone cannot provide sufficient tensile strength to resist bending stresses effectively. This is where

a high-volume fraction of fibers comes into play. The parameter M_{fiber} Quantifies the flexural capacity contribution due to dispersed steel fibers embedded throughout the concrete matrix. These fibers act as micro-reinforcement, bridging cracks, arresting crack propagation, and providing residual tensile strength even after initial cracking. Accordingly, the fiber contribution is expressed as:

$$M_{fiber} = (k_t V_f \sqrt{f_c'} + k_{fiber} f_{y.fiber}) b(h - a)\left(d - \frac{a}{2}\right) \quad (3)$$

where k_t is an empirically optimized coefficient representing fiber efficiency, V_f is the fiber volume fraction, h is the beam height, k_{fiber} is the fiber yield strength factor, and $f_{y.fiber}$ is the strength of fibers' material. The value of k_t= 0.0824 was obtained as the optimized tensile factor from the experimental database. The value of k_{fiber}=1.0×10^{-8} was found for the fiber yield strength contribution. The next step corresponds to the portion of the matrix in the flexural capacity measurement, which is provided by Eq. (4). In conventional reinforced concrete design, the tensile strength of the concrete matrix is often neglected due to its inherently brittle nature and low tensile capacity. However, in ductile HPC, this assumption is no longer valid. These advanced materials, due to their very low w/b ratios (typically 0.17–0.19) and dense binder-rich matrices, exhibit significantly improved tensile strength and post-cracking behavior, even before the addition of fibers. This contribution is especially important when the beam has low or very low reinforcement ratios, and the remaining tensile resistance must be shared among the matrix and fibers. As the ductile HPC mix contains high volumes of silica fume, fly ash, or other pozzolanic materials, which enhance the bond strength and toughness of the matrix, considering this parameter is essential for the calculation of M_n.

$$M_{matrix} = k_{ct} f_c' b(h - a)\left(d - \frac{a}{2}\right) \quad (4)$$

where k_{ct} is the optimized concrete matrix tension factor, which was found to be k_{ct}= 0.0109 according to the experimental database. As shown in Eqs. (3) and (4), the tensile strength of fiber and matrix can be described by Eqs. (5) and (6), respectively:

$$f_{t.f} = k_t V_f \sqrt{f_c'} \quad (5)$$

$$f_{ct} = k_{ct} f_c' \quad (6)$$

At the fourth step, the model uses a modified force equilibrium approach suited for low-reinforcement conditions. The stress block depth (a) is determined as:

$$a = \frac{A_s f_y}{\alpha_c f_c' b + \gamma (f_{t.f} + f_{ct}) b} \quad (5)$$

$$\alpha_c = \begin{cases} 0.85 & f_c' \le 60 \\ 0.85 - 0.002(f_c' - 60) & 60 < f_c' \\ \min 0.65 & \le 200 \end{cases} \quad (6)$$

$$\beta_1 = \begin{cases} 0.85 & f_c' \le 28 \\ 0.85 - 0.05\dfrac{(f_c' - 28)}{7} & 28 < f_c' \\ 0.60 & f_c' \ge 100 \\ & < 100 \end{cases} \quad (7)$$

where γ The weighting factor for fiber and matrix contribution, gamma=0.40, was found for the collected database. The parameters α_c and β_1 are stress block factors are used to approximate the compressive force distribution in concrete, particularly in the concrete compression zone. The parameter α_c as the stress block intensity factor, which represents the average stress in the concrete's compression zone. It scales the compressive strength to account for the nonlinear nature of the concrete stress-strain curve. This means that as concrete strength increases, α_c decreases to reflect the more brittle behavior of high-strength concrete. The parameter of β_1 as stress block depth factor defines the depth of the equivalent rectangular stress block as a fraction of the neutral axis depth. These two factors make it possible to simplify complex nonlinear concrete behavior into a tractable and conservative analytical model. The schematic illustration of the proposed model is presented in Figure 1. It is worth mentioning that k_{fiber} and k_{matrix} were proposed as a function of $(d - a/2)$ to be consistent with the M_{steel}. The k_1 and k_2 were derived from adjustments with experimental results. Identifying the impact location of the F_{fiber} and F_{matrix} forces are quite challenging and hinges on numerous factors; thus, adjustments based on empirical data were employed in this study. It is also important to note that the present study precisely separated the roles of fiber and matrix, which have not been exactly studied by previous investigations in ductile HPC beams. It is worth mentioning that normally, residual flexural tensile strength (f_R) is used in predicting the flexural capacity of HPC beams. However, this parameter was not measured in some databases mentioned in Table 1, accordingly, considering this parameter could provide some inaccuracy in the proposed model.

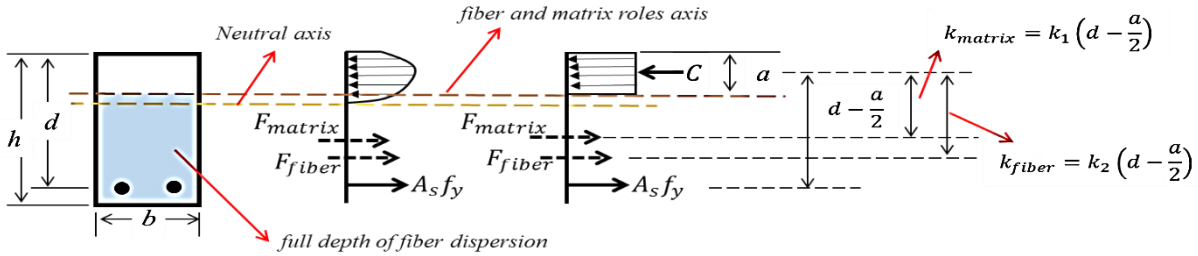

$$M_{matrix}=F_{matrix}k_{matrix}=b(h-a)(matrix\ equivalent\ formula)k_{matrix}$$
$$M_{fiber}=F_{fiber}k_{fiber}=b(h-a)(fiber\ equivalent\ formula)k_{fiber}$$

k_1 and k_2 were determined based on experimental adjustment

Figure 1: Schematic illustration of the proposed model for the ductile HPC beam.

Table 3.
Composition of ductile HPC mixture (kg/m^3)

Cement	SF	GGBFS	Silica Sand	w/b ratio	Micro steel fiber (volume fraction)
580	131	588	652	0.18	2.0%

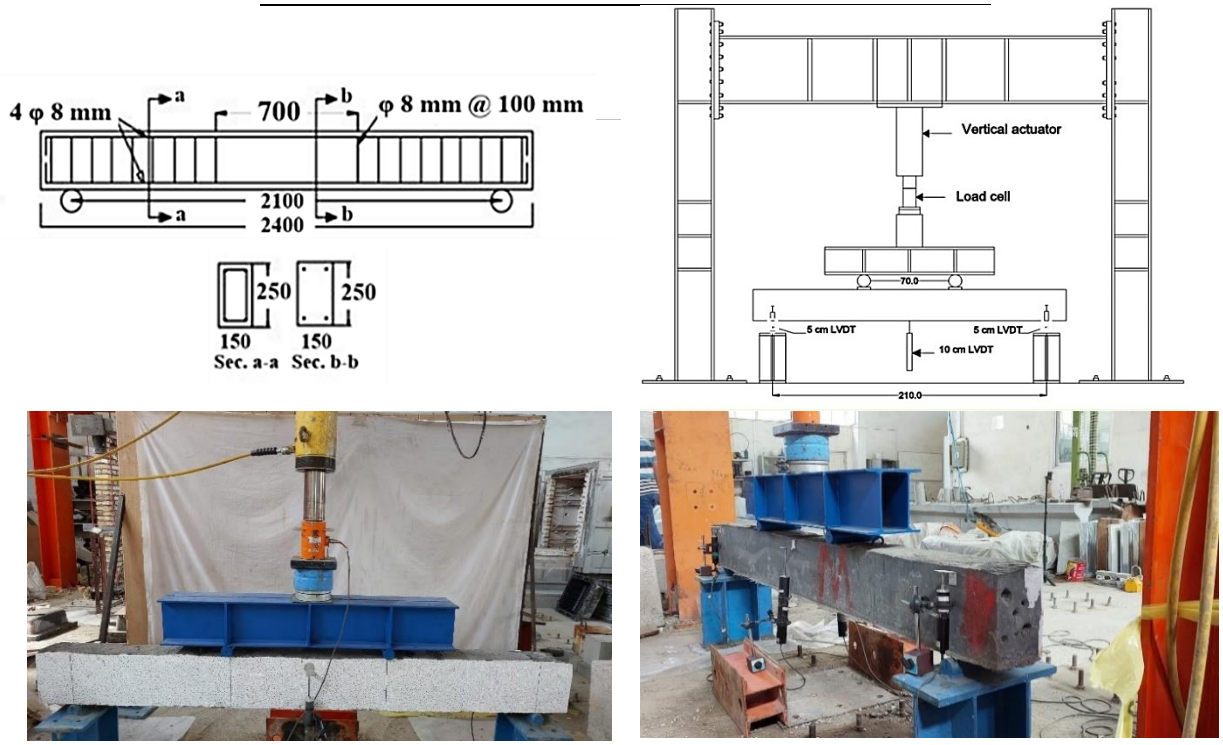

Figure 2: Details of the supplementary experimental program.

3. Experimental program

Ordinary Portland cement, ground granulated blast-furnace slag (GGBFS), and silica fume (SF) were utilized as binders for the ductile HPC mixture. As outlined in Table 3, the ductile HPC mixture features a w/b ratio of 0.18, a sand-to-binder (s/b) ratio of 0.50, and includes 2.0% micro steel fibers. The straight steel fibers employed had a length of 16 mm, an aspect ratio of 64, a tensile strength of 2720 MPa, and a modulus of elasticity of 210 GPa.

The addition of these fibers was intended to improve the mixture's tensile performance; nonetheless, this incorporation led to a decrease in the workability of the

mixture. A polycarboxylate superplasticizer (SP) was methodically included in all formulations to mitigate this problem. As illustrated in Figure 2, a large-scale ductile HPC beam with a very low reinforcement ratio (ρs=0.32%) was designed to prevent shear failure, adhering to the recommendations set forth by the Japan Society of Civil Engineers (JSCE) [9], to evaluate their flexural capacity. For the shear reinforcement, 8 mm stirrups were employed with a spacing of 100 mm, and to maintain the vertical position of the shear reinforcements (stirrups) within the shear zone, a minimal longitudinal reinforcement ratio of ρs=0.32%was considered, consisting of four 8 mm diameter reinforcing bars. The overall length of 2400 mm and section of 150×250 mm2 were considered for the ductile HPC beam, which had a height-to-width ratio of around 1.67. Regarding the large-scale flexural test, the rate of the universal machine was around 0.4 mm/min.

4. Results & Discussion

A comprehensive experimental database gathered in Table 1 was used in the present study to check the performance of the proposed model. This experimental database contains various groups of large-scale beams to cover the lower and upper bound of the proposed model containing bending moments, including (a) some samples with no reinforcement ratio ($M_{steel}=0$) but different type and volume fractions of fiber; (b) some samples with no low reinforcement ratio but no fibers ($M_{fiber}=0$). The existence of these groups within the experimental database can help prove that more accurate coefficients exist within the model, especially. k_1 and k_2. Integral absolute error (IAE) and the coefficient of variation (COV) are two metrics used to assess the accuracy of current models. The COV is defined as the ratio of predicted to experimental values, while the expression for IAE is described in Eq. (8). IAE exhibits greater sensitivity compared to COV. These criteria have been used by many studies in this field to check the accuracy of the predictive analytical models [19-20]. A dependable model should have a lower IAE value and COV factors nearly equal to one to be effective and precise in predicting flexural capacity.

$$IAE = \sum \frac{\sqrt{(Experimental - Predicted)^2}}{\sum Experimental} \quad (8)$$

The performance of the proposed model, as depicted in Figure 3, demonstrates its capability to accurately predict the flexural capacity of samples characterized by low reinforcement ratios and high fiber volume fractions. The model's accuracy is quantified using the IAE and COV.

The IAE, calculated using Eq. (8), is approximately 10.8%, with a COV of 1.04. This outcome reflects the robust performance of the proposed model, which is based on a dataset comprising 162 experimental samples from 16 distinct studies. Additionally, the individual contributions of steel, fibers, and the matrix were assessed through the proposed model to evaluate how alternative materials might replace the role of steel in large-scale beams with low reinforcement ratios. Consequently, the ratio of M_{steel}/M_n, M_{fiber}/M_n, and M_{matrix}/M_n were calculated and illustrated in Figure 4, which is called "bending moment contribution ratio (-)". This analysis demonstrates that reducing the reinforcement ratios increases the roles of fiber and matrix for handling the flexural capacity of ductile HPC beams. The difference between the roles of fiber and matrix separately in compensating for the reinforcement ratio role is clearly shown in Figure 4.

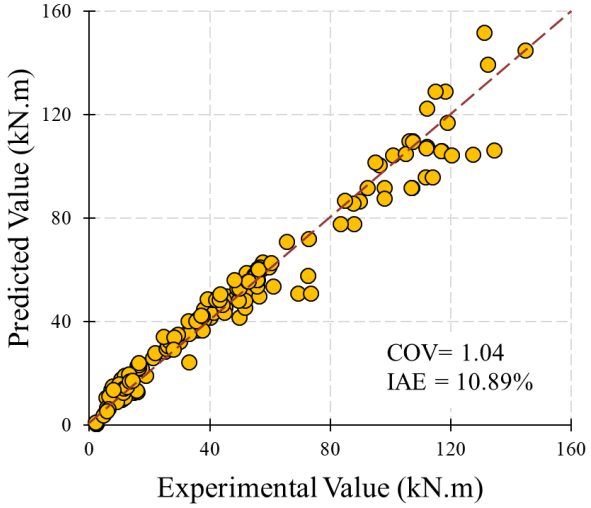

Figure 3: Performance of the proposed model for predicting the flexural capacity of ductile HPC beams with a low reinforcement ratio.

As mentioned, a supplementary experimental test was conducted to validate the proposed model. As shown in Figure 5(a), the tested large-scale ductile HPC beam had a bending moment capacity of 27.96 kN·m with clear ductile failure without unexpected failure due to the low reinforcement ratio. The tested beam had compressive strength of 100 MPa, direct tensile strength of 10 MPa, and splitting tensile strength of 12 MPa. High volume fraction of fibers within this ductile HPC beam (2.0%). The ductility index was calculated using the ratio of δ_u/δ_y, where δ_u and δ_y correspond to the initial and final displacement linked to 85% of the maximum force $0.85F_{max}$. As shown in Figure 5(a), the ductility ratio of 7.0 was measured for the tested beam. To check the performance of ductile HPC beam tested in the present study, various flexural capacity models proposed by

standards, including ACI 544.4R, JSCE-SF4, RILEM TC 162-TDF, and Fib Model Code 2010. Failure and crack propagation illustration of the tested beam is also shown in Figure 5(a). The performance of the proposed model in predicting the flexural capacity of the test beam is shown in Figure 5(b). The results showed that the proposed model precisely predicted the flexural capacity of the tested beam with 4.5% deviation. The analysis showed that reinforcement, fiber, and matrix have 8.1%, 10.4%, and 5.4% of the total bending moment, showing that fibers along with matrix compensate for the lack of adequate reinforcement within the ductile HPC beam, which can be a unique advantage of such concrete type. Moreover, the analysis showed that the fiber role is higher than reinforcement and matrix for the tested beam. Accordingly, the results show that the proposed model is a pioneer model to precisely separate the role of reinforcement (steel and fiber) within the ductile HPC beam on tolerating bending moment.

As mentioned in Table 4, a parametric study was also conducted in the present study using statistical analysis through Minitab software to discuss the sensitivity analysis of the input features in this flexural model. The ratio of M_{fiber}/M_n and $M_{matrix}/M_n$was used as "fiber and matrix roles, respectively" in this statistical analysis. Main effect plots of roles are shown in Figure 6. The provided analysis presents a comparison of how various input parameters affect the roles of fibers and matrices. As the volume fraction of fiber increases, the fiber role enhances, demonstrating that a higher proportion of fibers in the composite directly boosts their reinforcing capacity. In contrast, a rise in the w/b ratio leads to a slight reduction in the fiber role, suggesting that an increased water content may compromise the fiber-matrix interface, thereby diminishing the effectiveness of the fibers. The reinforcement ratio (ρ_s) has a significant negative impact on the fiber role, indicating that using an adequate reinforcement ratio within the beam section can be dominant in tolerating bending moment, thereby reducing both the roles of fiber and matrix. Furthermore, a size effect coefficient was also used as an input feature of the sensitivity analysis, which was calculated as $1/\sqrt{d}$, where d is the effective depth of the beam section. The size effect coefficient shows a moderate negative influence, meaning that an increase in the size coefficient slightly reduces the effectiveness of fibers in mechanical performance, likely due to limitations in stress transfer or distribution. Likewise, a rise in the fiber aspect ratio leads to a slight decline in fiber efficiency, implying the existence of an optimal aspect ratio, beyond which fibers may become less effective due to potential aggregation or poor stress transfer. On the other hand, the fiber yield strength positively affects the fiber role, signifying that fibers with greater strength enhance the reinforcing efficiency directly. Regarding the matrix role, the pattern differs: an increase in fiber volume fraction significantly diminishes the matrix role, indicating that as fiber content increases, the load-bearing function shifts from the matrix to the fibers. The w/b ratio also markedly reduces the matrix's contribution, likely due to matrix weakening associated with higher porosity and decreased strength at elevated w/b ratios.

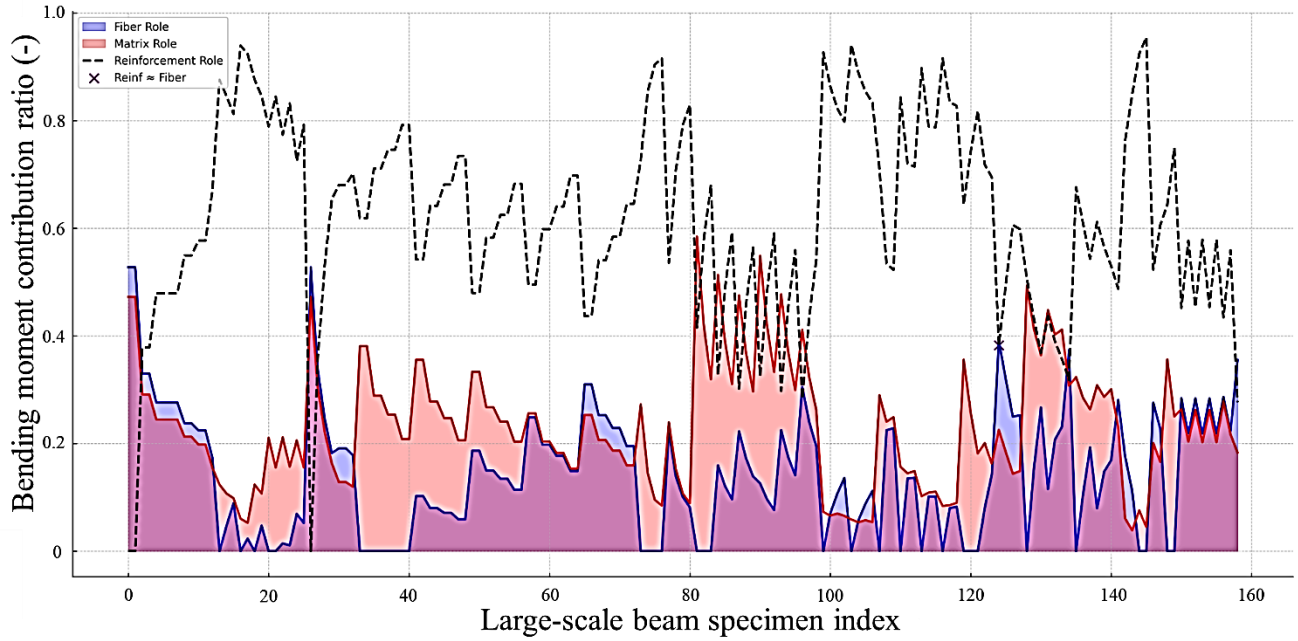

Figure 4: Portions of variables in predicting the flexural capacity of ductile HPC beams with low reinforcement ratios.

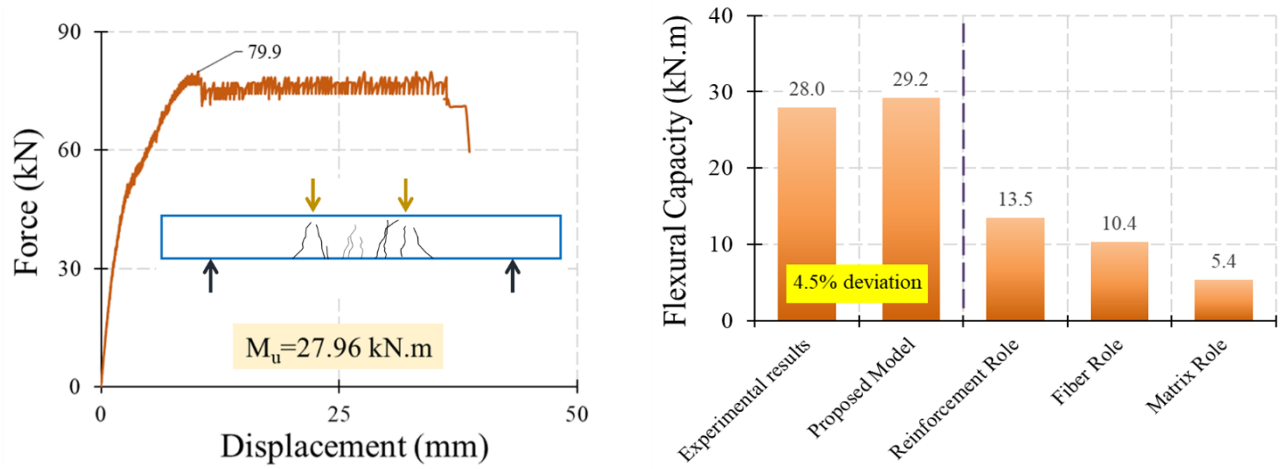

(a) (b)

Figure 5: Performance of the proposed model with supplementary experimental results: (a) experimental load-displacement curve; (b) compared with the proposed model.

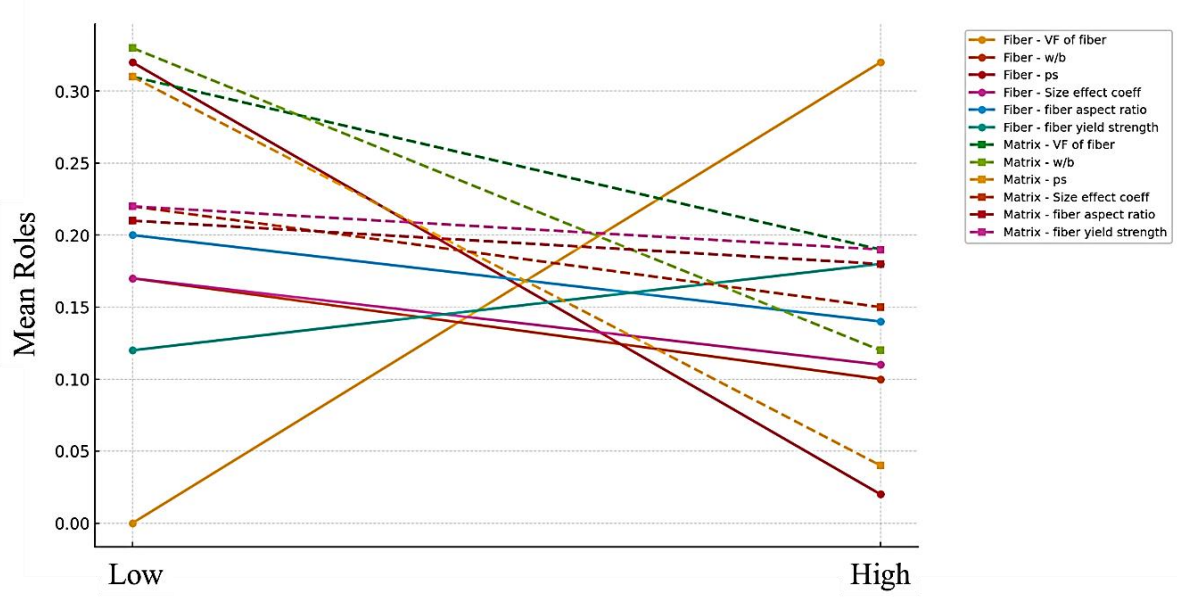

Figure 6: Main effect plots for fiber and matrix roles.

Table 4.

Statistical ANOVA analysis of the fiber and matrix role.

Terms		DF	Adj SS	Adj MS	F-value	P-value	VIF
Fiber Role	V_f	1	0.74	0.74	234.46	0.000	1.59
	ρ_s	1	0.313	0.314	99.84	0.000	1.22
	Size effect	1	0.0093	0.0093	2.96	0.088	1.24
	Fiber strength	1	0.0061	0.0061	1.95	0.165	2.66
	Fiber aspect ratio	1	0.0051	0.0051	1.61	0.206	2.00
	w/b	1	0.0086	0.0086	2.74	0.100	1.71
Matrix Role	V_f	1	0.138	0.138	39.77	0.000	1.59
	ρ_s	1	0.819	0.819	235.76	0.000	1.22
	Size effect	1	0.017	0.017	4.83	0.030	1.24
	Fiber strength	1	0.002	0.002	0.69	0.407	2.66
	Fiber aspect ratio	1	0.000	0.000	0.05	0.828	2.00
	w/b	1	0.481	0.481	138.40	0.000	1.71

Similarly, a rise in reinforcement ratio (ρ_s) greatly lowers the matrix contribution. An increase in the size effect coefficient slightly diminishes matrix effectiveness, suggesting limitations in the matrix's capacity to accommodate stress due to larger structural influences. Additionally, the fiber aspect ratio presents only minor negative effects, indicating that the matrix role is not heavily influenced by fiber geometry. Finally, the fiber yield strength has a negligible impact on the matrix role, suggesting that the strength characteristics of fibers mainly affect fiber efficiency without significantly altering the core load-bearing properties of the matrix. It is worth mentioning that the high volume of powders 9typically cement, SF, FA, and GGBFS) play a major role in matrix contribution, which is totally different from the fiber role's constitution.

The Pareto charts obtained from the statistical analysis of fiber and matrix roles are shown in Figure 7. A Pareto chart is a statistical analysis that combines a bar and line graph to display the relative importance of different factors in a dataset, where the bars represent individual values in descending order and the line shows the cumulative total. In statistical analysis, particularly in quality control and experimental design, it helps identify the "vital few" factors that contribute most significantly to an outcome. Based on Pareto charts (Figure 7), for fiber role, the most statistically significant effects—those exceeding the reference line—include AB (the interaction between volume fraction of fiber and ρ_s), BB (the quadratic effect of ρ_s), and CC (the quadratic effect of size effect coefficient), indicating that these terms have a dominant influence on the fiber role in total bending moment. The strong presence of AB suggests that the combined effect of the volume fraction of fiber and ρ_s is more impactful than their contributions, while BB and CC highlight nonlinear relationships, meaning that extreme values of ρ_s and size effect coefficient may disproportionately affect fiber performance. Additionally, AC (interaction between volume fraction of fiber and size effect coefficient) and AD (interaction between fiber volume fraction and fiber yield strength) also appear notable, though slightly less pronounced. For Matrix Role, the dominant effects are BB (the quadratic effect of ρ_s), showing that the reinforcement ratio of section controls the efficiency of matrix role in the proposed flexural strength model. The appearance of CC (the quadratic effect of the size effect coefficient), and FF (the quadratic effect of w/b ratio) imply that fiber volume fraction and fiber yield strength may also play a role in matrix behavior, hinting at cross-dependent mechanisms between fiber and matrix phases. The absence of certain main effects (e.g., A, B, C alone) in the most significant terms suggests that interactions and quadratic effects are more critical than individual linear factors in your system.

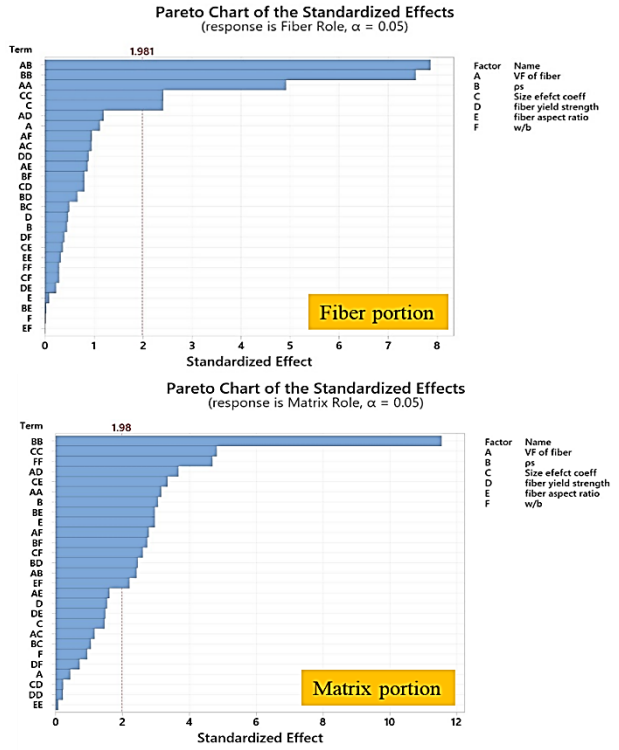

Figure 7: Pareto charts of fiber and matrix roles.

Response surface analysis from "Design of Experiments (DOE)" for fiber and matrix roles is illustrated in Figure 8. Regarding the fiber role, the contour plot demonstrates that the volume fraction of fibers plays the most dominant parameter when the $\rho_s < 0.01$, where a very low reinforcement ratio is considered in ductile HPC beams. Moreover, the analysis depicts that the existence of high-volume fraction fiber with low number aspect ratio has no promising influence on the fiber role, while fiber aspect ratio ranging from 400 to 800 guarantees a high effect of fiber volume fraction. Similarly, fiber strength is also critical so that a high-volume fraction of fibers cannot be efficient for fibers with a strength lower than 2000 MPa. Based on the response surface contour, the highest impact of fiber volume fraction in the fiber role formula is also obtained for the size effect factor higher than 0.090. However, the analyses depict that the variation of the w/b the ratio has the lowest influence on the fiber role predicting formula. Regarding matrix role, the variation of fiber volume fraction also has a minor influence on the matrix role, while using the lowest content of reinforcement ($\rho_s < 0.02$) has a considerable impact. Also, using a fiber aspect ratio lower than 300 provides a situation that. $M_{matrix} > M_{fiber}$. Similarly, for a case where the matrix role is dominant over the fiber role, the fiber strength should be lower than 1500 MPa, as illustrated in Figure 8. In the case of the size effect value lower than 0.07, along with $w/b \leq 0.20$, the matrix role is dominant as

compared to the fiber role for ductile HPC beams containing a low reinforcement ratio.

The overlaid contour plots from DOE for fiber and matrix roles are depicted in Figure 9. The domain of 0.20-0.52 for fiber role was selected for this optimization analysis. The analysis showed that a reinforcement ratio lower than 0.015 and a fiber volume fraction of 2.0% can result in the maximum performance of fibers in achieving the highest M_{fiber}. Regarding the size effect parameter and fiber strength, no clear trend was observed, while the current observation confirmed that a size effect parameter higher than 0.09 and fiber strength higher than 2500 MPa can generate the highest fiber role in the total bending moment predicting model. Regarding the w/b ratio, the analysis clearly showed that the addition of fibers in $w/b >$ 0.40 almost has no impact on the bending moment. Similarly, as shown in Figure 9, a fiber aspect ratio higher than 400 causes the minor influence of fibers within the bending moment calculation. A similar range of 0.2-0.58 was selected for optimization analysis of the matrix role. The analysis showed that fiber yield strength higher than 2000 MPa and reinforcement ratio higher than 0.01 increase the non-feasible region, meaning that the M_{matrix} can be ignored in the calculation of total bending moment. Furthermore, the analysis showed that for $w/b < 0.3$ and $100 < fiber\ aspect\ ratio < 300$, the value of M_{matrix} should be considered in the total bending moment calculation.

The main question is whether, by variation of input features, the fiber or the matrix is dominant in compensating reinforcement within ductile HPC beams. To answer this question, the boxplots are illustrated in Figure 10. Regarding fiber content, dominantly higher fiber volume fractions correlate strongly with cases where the fiber role exceeds the matrix role. The analysis of the reinforcement ratio (ρ_s) showed that slightly lower

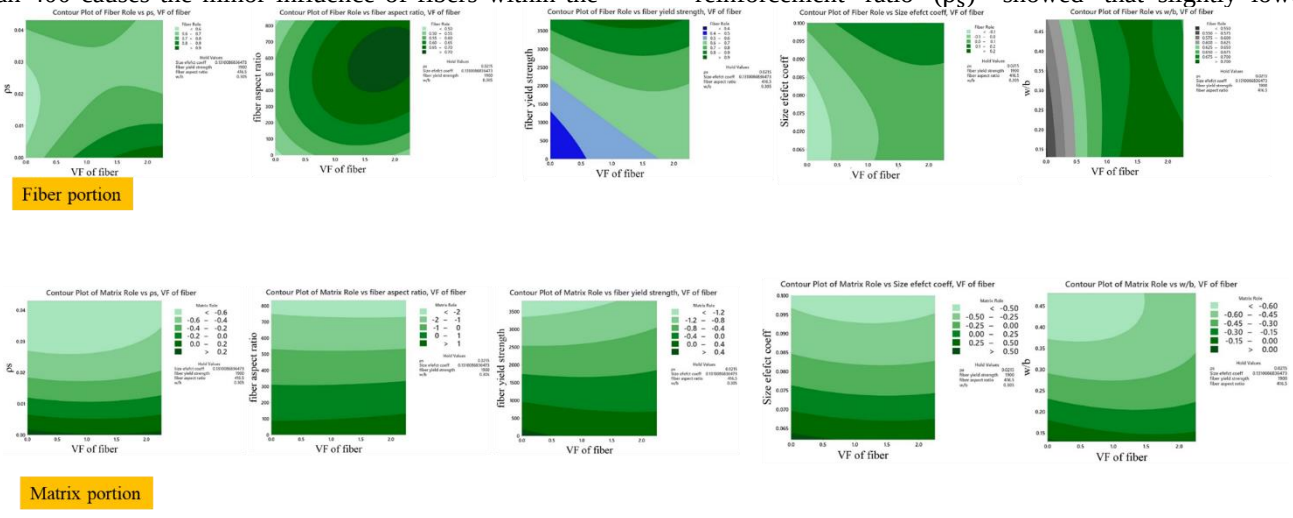

Figure 8: Response surface analysis from DOE for fiber and matrix roles.

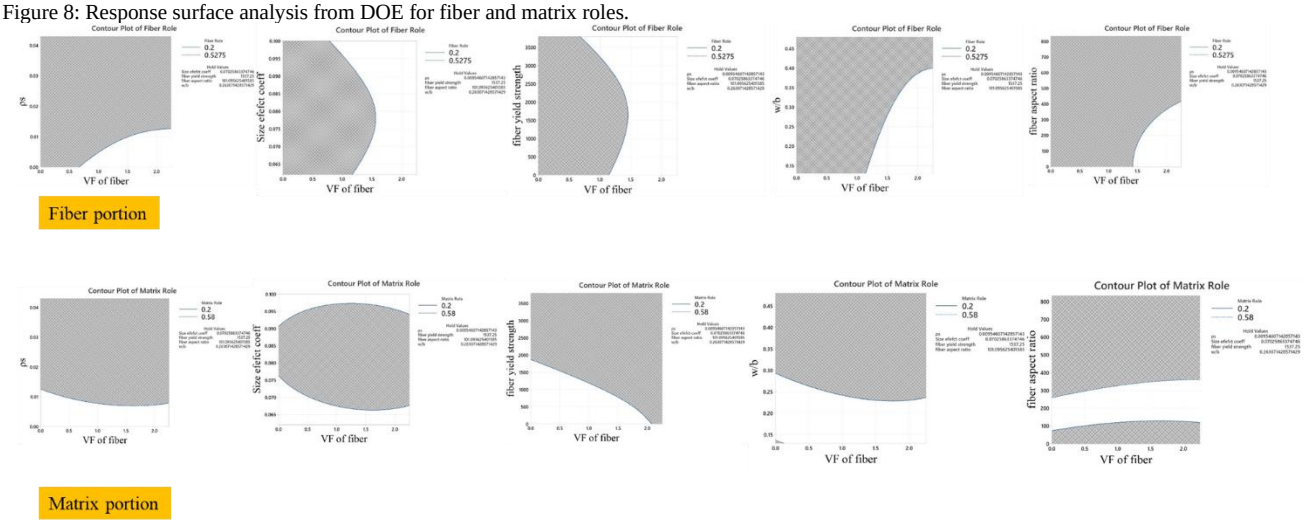

Figure 9: Overlaid contour plot from DOE for fiber and matrix roles.

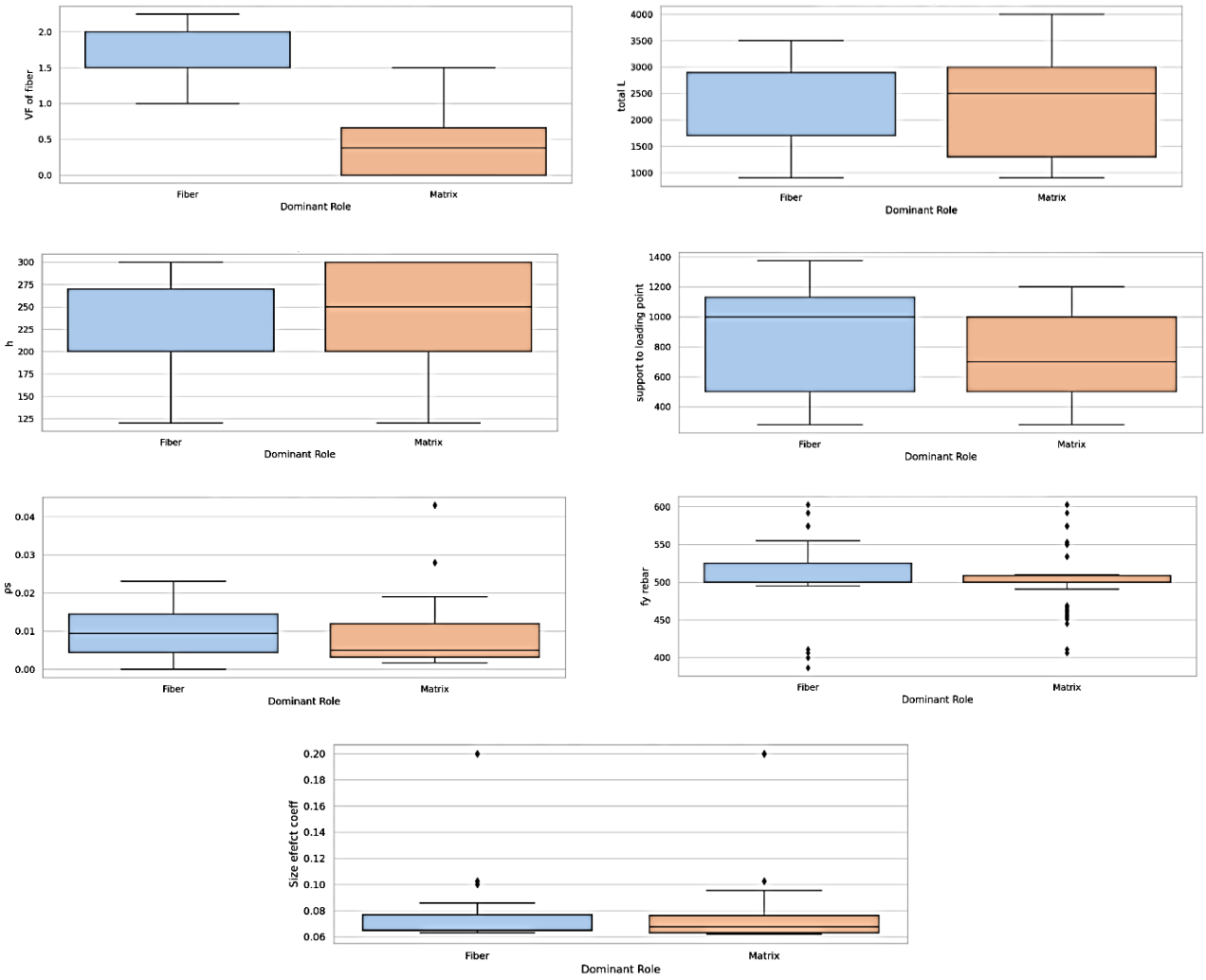

Figure 10: Results of box plots illustrating the distribution of input parameters for the Fiber and Matrix roles.

reinforcement ratios tend to favor fiber dominance. Also, the analysis depicted that slightly shorter specimen lengths tend to favor fiber dominance. Moreover, lower size effect coefficients slightly favor the fiber role, indicating fibers are more effective at smaller scales. Generally, the analysis confirmed that the strongest factor differentiating fiber and matrix dominance is the fiber volume fraction.

A comparison between predicting models suggested by various concrete design codes and the proposed model of the presented study is conducted and shown in Table 5. The bending moment of the ductile HPC beam tested in the present study was selected as the criterion for comparing the efficiency of the models. Based on the deviation analysis, the current design codes significantly underestimate the flexural capacity of ductile HPC beams, with deviation ranging from -20.0% to -43.57%, while the proposed model precisely predicts the bending moment with +4.25% deviation. Among the proposed models, the analysis depicts that JSCE-SF4 (2002) showed the lowest deviation from the experimental results, while ACI 544.4R has the highest deviation. The high accuracy of the proposed model in the present study is a promising finding for use in the design codes in predicting the flexural capacity of HPC beams.

Table 5.
Performance of predicting equations compared to the experimental beam

	Models	Predicted (kN.m)	Deviation from experiment (%)
Design Codes	ACI 544.4R	15.8	-43.57
	JSCE-SF4 (2002)	22.4	-20.0
	RILEM TC 162-TDF	18.9	-32.5
	Fib Model Code (2010)	20.2	-27.86
	Proposed model	29.2	+4.28

5. Conclusions

A novel analytical approach was followed by the present study to propose a unique predicting flexural capacity model for large-scale ductile HPC (or other fiber-reinforced concrete types) beams containing almost negligible reinforcement content. A comprehensive experimental database containing 162 datasets was gathered from the literature to determine the performance of the proposed model. Moreover, a supplementary experimental program containing one large-scale ductile HPC beam was produced to check the accuracy of the model. The results showed that the proposed bending model has IAE=10.8% and COV=1.04, which clearly shows the high accuracy of the proposed model compared to the experimental database (162 experimental large-scale beam tests). Furthermore, comparing the experimental result of the tested beam and the proposed model showed a 4.5% deviation, which confirms the performance of the flexural capacity formulation. A parametric statistical analysis using Minitab software was also conducted to check the influence of critical parameters affecting the fiber and matrix role. Different input features were considered in this statistical sensitivity analysis. Generally, the parametric study emphasized that the volume fraction of fiber, w/b ratio of concrete mixture, reinforcement ratio of beam, fiber strength (or type), and fiber aspect ratio have a considerable impact on the role of fiber and matrix in compensating the flexural capacity required due to the inadequate reinforcement ratio. Also, the size effect parameter was found to be important in the proposed model. More experimental studies are required for future research to validate the efficiency of the proposed model, especially for different types of HPC mixtures. Moreover, only monotonic loading was considered for the proposed flexural capacity model, while more analytical work should be performed by future studies to extend the proposed model for cyclic conditions.

Notations

A_s	area of reinforcement in the beam section
b	beam width
d	Effective depth of the beam section
f_c'	concrete compressive strength
f_{ct}	matrix tensile strength
f_{ctm}	cracking control limit strength
f_R	Residual flexural tensile strength
f_y	yield strength of reinforcement
$f_{y.fiber}$	strength of fibers' materials
$f_{t.f}$	fiber residual tensile strength
h	beam height
k_t	optimized fiber tensile strength factor
k_{ct}	optimized concrete matrix tension strength factor
k_{fiber}	fiber yield strength factor
M_n	flexural capacity of the beam
M_{steel}	portion of reinforcement in flexural capacity
M_{fiber}	portion of reinforcement in flexural capacity
M_{matrix}	portion of the matrix in flexural capacity
V_f	fiber volume fraction (%)
α_c	stress block intensity factor
β_1	stress block depth factor
a	neutral axis depth
γ	weighting factor for fiber & matrix contribution to neutral axis
ρ_s	reinforcement ratio of the beam section

References

[1] Yang, In Hwan, Changbin Joh, and Byung-Suk Kim. "Structural behavior of ultra-high performance concrete beams subjected to bending." Engineering Structures 32.11 (2010): 3478-3487. https://doi.org/10.1016/j.engstruct.2010.07.017

[2] Meda, A., F. Minelli, and G.A. Plizzari. "Flexural behaviour of RC beams in fibre reinforced concrete." Composites Part B: Engineering 43.8 (2012): 2930-2937. https://doi.org/10.1016/j.compositesb.2012.06.003.

[3] Kamal, M., M. Safan, Z. Etman, and R. Salama. "Behavior and strength of beams cast with ultra high strength concrete containing different types of fibers." HBRC Journal 10.1 (2014): 55-63. https://doi.org/10.1016/j.hbrcj.2013.09.008.

[4] Abbas, S., A.M. Soliman, and M.L. Nehdi. "Exploring mechanical and durability properties of ultra-high performance concrete incorporating various steel fiber lengths and dosages." Construction and Building Materials 75 (2015): 429-441. https://doi.org/10.1016/j.conbuildmat.2014.11.017.

[5] Yoo, Doo-Yeol, Nemkumar Banthia, and Young-Soo Yoon. "Experimental and numerical study on flexural behavior of UHPFRC beams with low reinforcement ratios." (2016). http://hdl.handle.net/1807/75095.

[6] Yoo, Doo-Yeol and Doo-Yong Moon. "Effect of steel fibers on the flexural behavior of RC beams with very low reinforcement ratios." Construction and Building Materials 188 (2018): 237-254. https://doi.org/10.1016/j.conbuildmat.2018.08.099.

[7] Cardoso, D.C., R.C. Silva, J.P.C. Rodrigues, and A.T. Marques. "Influence of steel fibers on the flexural behavior of RC beams with low reinforcing ratios: Analytical and experimental investigation." Composite Structures 222 (2019): 110926. https://doi.org/10.1016/j.compstruct.2019.110926.

[8] Abbasi Parvin, Younes, Mohammad Ali Hadianfard, Amirhossein Gholamrezaei, and Sajad Bagheryan. "Flexural behavior of UHPC beams reinforced with macro-steel fibers and different ratios of steel and GFRP bars." Journal of Rehabilitation in Civil Engineering 12.2 (2024): 41-57. https://doi.org/10.22075/jrce.2023.28070.1695.

[9] JSCE. "Standard Specifications for concrete structures." Japanese Society for Civil Engineering (JSCE) (2010). https://www.jsce-int.org/system/files/JGC15_Standard_Specifications_Design_1.0.pdf.

[10] Yoo, Doo-Yeol and Young-Soo Yoon. "Structural performance of ultra-high-performance concrete beams with different steel fibers." Engineering Structures 102 (2015): 409-423. https://doi.org/10.1016/j.engstruct.2015.08.029.

[11] Singh, M., I. Sheikh, M. Ali, M. Shariq, and A. Baqi. “Experimental and numerical study of the flexural behaviour of ultra-high performance fibre reinforced concrete beams.” Construction and Building Materials 138 (2017): 12-25. https://doi.org/10.1016/j.conbuildmat.2017.02.002.

[12] Hasgul, U., K. Turker, A. Birol, and A. Yavas. “Flexural behavior of ultra-high-performance fiber reinforced concrete beams with low and high reinforcement ratios.” Structural Concrete 19.6 (2018): 1577-1590. https://doi.org/10.1016/j.conbuildmat.2017.02.002.

[13] Gümüş, M. and A. Arslan. “Effect of fiber type and content on the flexural behavior of high-strength concrete beams with low reinforcement ratios.” Structures (2019). https://doi.org/10.1016/j.istruc.2019.02.018.

[14] Liu, S., W. Wang, L. Mao, and Z. Li. “Flexural load-deflection performance of polyvinyl alcohol fiber reinforced cementitious composite beams.” Construction and Building Materials 223 (2019): 1135-1144. https://doi.org/10.1016/j.conbuildmat.2019.07.215.

[15] Turker, K., U. Hasgul, A. Birol, and A. Yavas. “Hybrid fiber use on flexural behavior of ultra high performance fiber reinforced concrete beams.” Composite Structures 229 (2019): 111400. https://doi.org/10.1016/j.compstruct.2019.111400.

[16] Conforti, A., R. Zerbino, and G. Plizzari. “Assessing the influence of fibers on the flexural behavior of reinforced concrete beams with different longitudinal reinforcement ratios.” Structural Concrete 22.1 (2021): 347-360. https://doi.org/10.1002/suco.201900575.

[17] Chen, H.-J., W.-C. Huang, C.-C. Huang, and Y.-W. Chan. “Flexural behavior of ultra-high-performance fiber-reinforced concrete beams after exposure to high temperatures.” Materials 14.18 (2021): 5400. https://doi.org/10.3390/ma14185400.

[18] Jin, H., F. Li, and D. Hu. “Research on the flexural performance of reinforced engineered cementitious composite beams.” Structural Concrete 23.4 (2022): 2198-2220. https://doi.org/10.1002/suco.202100012.

[19] Mousavi, S., M. Dehestani, and S. Mousavi. “Bond strength and development length of glass fiber-reinforced polymer bar in unconfined self-consolidating concrete.” Journal of Reinforced Plastics and Composites 35.11 (2016): 924-941. https://doi.org/10.1177/0731684416632930.

[20] Wu, Y. F. and X. M. Zhao. “Unified bond stress–slip model for reinforced concrete.” Journal of Structural Engineering 139.11 (2013): 1951-1962. https://doi.org/10.1061/(ASCE)ST.1943-541X.0000747.